JAAS

PAPER

View Article Online
View Journal | View Issue

Cite this: *J. Anal. At. Spectrom.*, 2024, **39**, 2207

Received 18th April 2024
Accepted 9th July 2024

DOI: 10.1039/d4ja00147h

rsc.li/jaas

A potential natural chalcopyrite reference material for *in situ* copper, iron, and sulfur isotope measurements†

Lie-Wen Xie, *[a] Hong-Rui Fan,[a] Hui-Min Yu,[b] Chao Huang,[a] Lei Xu,[a] Yue-Heng Yang,[a] Shi-Tou Wu[a] and Hao Wang[a]

Chalcopyrite has been extensively utilized for tracing geological processes through its Cu, Fe and S isotopic compositions. However, the matrix-matched reference materials for micro-analysis are lacking. This study focused on assessing the feasibility of a natural chalcopyrite specimen (IGGCcp-1) as a matrix-matched reference material for *in situ* micro-analysis of Cu, Fe, and S isotopes. Electron probe microanalysis validated the uniform distribution of major elements within chalcopyrite grains, with no evidence of growth zoning. Random spot isotopic measurements using LA-MC-ICP-MS demonstrated remarkable consistency in δ^{65}Cu, δ^{56}Fe and δ^{34}S. These results indicated that the IGGCcp-1 specimen exhibited its suitability as a reference material. Using SN-MC-ICP-MS technique, the δ^{65}Cu value was accurately determined to be 0.43 ± 0.05‰ (2S, $N = 30$). Furthermore, the $\delta^{56}\text{Fe}_{\text{IRMM-014}}$ and $\delta^{57}\text{Fe}_{\text{IRMM-014}}$ values were recorded as −0.24 ± 0.04‰ (2S, $N = 18$) and −0.36 ± 0.09‰ (2S, $N = 18$), respectively. Additionally, the $\delta^{34}\text{S}_{\text{VCDT}}$ measurement, performed with EA-IRMS, yielded a value of −0.28 ± 0.60‰ (2S, $N = 10$). These precisely measured isotope ratios established the recommended reference values for the IGGCcp-1 sample in future applications of Cu, Fe, and S isotope micro-analysis.

Introduction

Chalcopyrite ($CuFeS_2$) is the most prevalent copper-bearing mineral found in diverse copper deposits, including porphyry copper–molybdenum (gold) deposits and skarn iron–copper deposits.[1–4] Previous research studies have shown that chalcopyrite samples exhibit a wide variability in their isotopic compositions. For instance, in the Schwarzwald mining district, chalcopyrite in the hydrothermal vein exhibits a substantial δ^{65}Cu range spanning from −2.92‰ to 0.49‰.[5] Meanwhile, in the late Carboniferous Baogutu reduced porphyry copper deposit located in the western Junggar Terrane, northwestern China, the δ^{56}Fe values of chalcopyrite vary between −0.23‰ and 0.57‰.[3] Similarly, S isotopes can vary considerably, as shown by the difference between Nifty (−3.58‰ in δ^{34}S)[6] and TC1725 (12.78‰ in δ^{34}S).[7] The Cu–Fe–S isotopic fingerprints of the chalcopyrite can serve as powerful indicators, offering valuable insights into metal provenance, fluid chemistry, mineral formation processes, and ambient conditions, thereby establishing chalcopyrite as a superior multi-isotope tracer.[1–5]

Additionally, chalcopyrite, characterized by its rich concentration of Cu, Fe and S elements, is an excellent candidate for isotopic composition analysis using *in situ* micro-analytical techniques, such as the laser ablation multi-collector inductively coupled plasma mass spectrometry (LA-MC-ICP-MS) for Cu–Fe–S isotopic measurement and the secondary ion mass spectrometry (SIMS) for S isotopic measurement.[6–9] Researchers can achieve precise measurements of Cu–Fe–S isotopic ratios within individual chalcopyrite grains or specific areas of interest. These techniques provide high spatial resolution analyses, enabling a thorough investigation of isotopic spatial variations within this mineral. However, numerous studies have substantiated the necessity and effectiveness of using matrix-matched reference materials to correct for the mass fractionation and mitigate matrix effects during the entire LA-MC-ICP-MS or SIMS analytical process, such as Fang *et al.* (2023)[10] and Li *et al.* (2020).[11]

The attainment of isotopically homogeneous matrix-matched chalcopyrite reference materials can be achieved either through the synthesis from ultra-fine chalcopyrite powders or the identification within naturally occurring chalcopyrite samples. Among these strategies, the synthesis from ultra-fine powders presents a relatively simple and eminently scalable production method, particularly conducive to large-scale manufacturing needs. This includes procedures such as

---

[a] *State Key Laboratory of Lithospheric Evolution, Institute of Geology and Geophysics, Chinese Academy of Sciences, P. O. Box 9825, Beijing 100029, P. R. China*

[b] *CAS Key Laboratory of Crust-Mantle Materials and Environments, School of Earth and Space Sciences, University of Science and Technology of China, Hefei 230026, P. R. China*

† Electronic supplementary information (ESI) available. See DOI: **https://doi.org/10.1039/d4ja00147h**

compacting ultra-fine chalcopyrite powder, exemplified by PSPT-1 for S isotopic assessments;[12] melting chalcopyrite powder at temperatures of 1000 °C, as seen in chalcopyrite glass YN411-m for S isotopic measurements;[13] employing the plasma-activated sintering technique, illustrated by PAS-Cpy which caters to both S and Fe isotopic analyses;[14] and blending chalcopyrite powder with epoxy resin, like the standard RPP-GBW07268 designed for S isotopic determinations.[15]

However, it is crucial to recognize that the laser ablation properties of the synthetic samples prepared using a combination of ultra-fine powders would be different from those of natural samples. For instance, a recent study by Feng *et al.* (2022) revealed that the Fe signals obtained from ablating compressed powder pellets were conspicuously stronger compared to natural samples.[14] This disparity underscores the significant influence of matrix effects during laser ablation, implying the need for rigorous scrutiny of experimental results calibrated using synthetic samples to ensure accuracy and reliability.[14]

Despite the inherent challenge in identifying natural chalcopyrite samples that exhibit isotopic homogeneity across Cu, Fe, and S elements, thereby qualifying as optimal matrix-matched reference materials, several naturally occurring chalcopyrite reference materials and custom-made laboratory standards have been successfully developed. These include GC and Cpy-1,[13] TC1725,[7] Nify-b,[6] HTS4-6 and CPY-1,[11] Norilsk and Trout Lake,[16] OPM,[17] Ll-Cpy,[18] and IGSD,[19] which have been utilized for S isotopes measurement. For Cu isotope analysis, notable examples encompass 14ZJ12-1, JGZ-29, and JGZ-78,[20] T1725,[7] Ll-Cpy,[18] and TQ-Ccp.[10] As for Fe isotope analysis, researchers have employed Tianyu-Ccp[9] and Ll-Cpy.[18] Despite these advancements, however, there remains a scarcity of naturally occurring chalcopyrite samples that have undergone isotopic characterization for Cu, Fe, and S, hindering their potential as comprehensive, multipurpose reference materials for simultaneous or respective Cu–Fe–S isotopic analyses.

This study introduced a naturally occurring chalcopyrite specimen as a promising reference material in micros-analyses of Cu, Fe, and S isotopic composition. To assess its isotopic homogeneity across Cu, Fe, and S, the sample underwent meticulous spot analyses utilizing femtosecond laser ablation multi-collector inductively coupled plasma mass spectrometry (fs-LA-MC-ICP-MS). Following this, the precise determination of Cu and Fe isotopic compositions was carried out separately *via* solution nebulization multi-collector inductively coupled plasma mass spectrometry (SN-MC-ICP-MS), while S isotopic compositions were measured using elemental analyzer-isotope ratio mass spectrometry (EA-IRMS).

Sample description and preparation

In this study, we carefully selected chalcopyrite grains from a chalcopyrite-bearing ore specimen depicted in Fig. 1a, designating this natural chalcopyrite sample as 'IGGCcp-1' for subsequent analysis and potential use as a reference material. The sample was collected from the Hongtoushan copper–zinc deposit with a total reserve of 0.5 Mt Cu at a grade of 1.5–1.8 wt% and 0.7 Mt Zn at a grade of 2.0–2.5 wt% in the Qingyuan greenstone belt, North China Craton. The Hongtoushan deposit was the oldest Archean volcanogenic massive sulfide (VMS) deposit in China, and suffered late metamorphic remobilization.[21] Under the regional high-grade metamorphism, the deposit had undergone intensive deformation and remobilization, forming vertical "ore pillar" and ore shoots enriched in Cu, Zn, and Ag elements.[22] The sample collected from "ore pillar" or massive ore at Hongtoushan was dominated by chalcopyrite

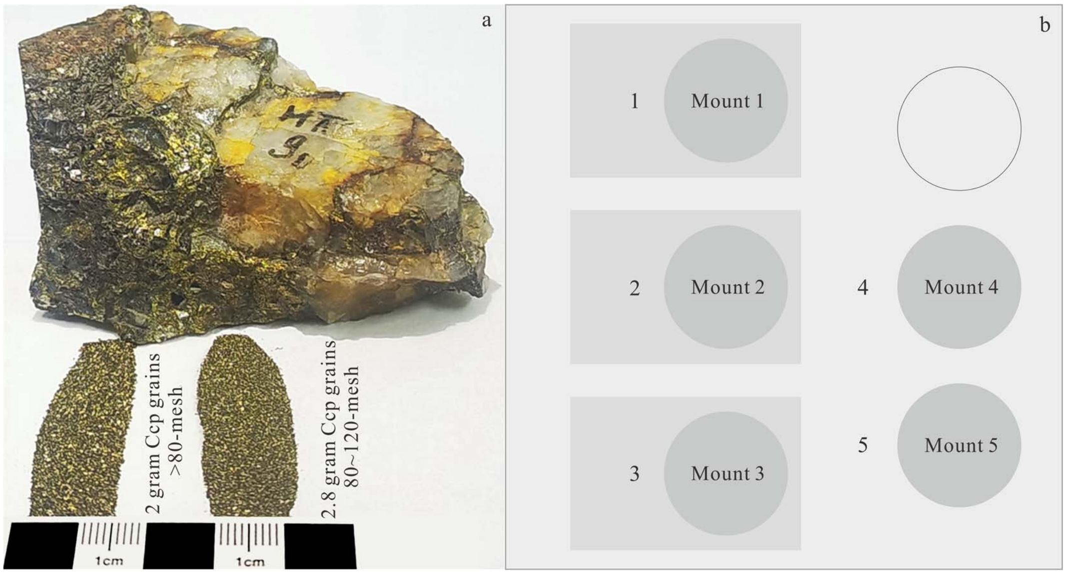

Fig. 1 The IGGCcp-1 chalcopyrite sample investigated in this study. (a) A segment of the chalcopyrite hand specimen along with two different grain sizes manually extracted from it have been included; (b) an illustrative representation of the sample tray highlights the locations of mount 1, mount 2, mount 3, mount 4, and mount 5.

and pyrrhotite, with a trace amount of sphalerite, magnetite, anhydrite, and galena.

To ensure randomness and representativeness, grains of varying dimensions from the natural chalcopyrite sample IGGCcp-1 were systematically chosen and embedded in four separate 1-inch epoxy resin mounts, designated as mounts 1 through 4. Additionally, the IGGCcp-1 chalcopyrite grains, the IGGPy-1 pyrite grains and an in-house chalcopyrite standard grains-designated as IGGCcp-2, whose comprehensive details can be found in the ESI,† were embedded into mount 5.

All five mounts were meticulously polished to achieve a flat and smooth surface that facilitated effective laser ablation analysis. Subsequently, they were positioned within their corresponding sample mount cavities numbered 1 through 5 on the sample tray of the TV2 sample cell, as illustrated in Fig. 1b.

Analytical methods

Electron probe microanalysis (EPMA)

Elemental chemical compositions were precisely quantified utilizing a state-of-the-art CAMECA SXFiveFE electron probe micro-analyzer (EPMA) located at the Institute of Geology and Geophysics, Chinese Academy of Sciences (IGGCAS). Under operation, the instrument maintained an acceleration voltage of 20 kilovolts, a finely-tuned probe current of 30 nanoamperes, and a sharply-focused beam for enhanced accuracy and resolution. For calibration purposes, a diverse array of reference materials was used, which included pure metal standards such as Co, Ni, and Cu, representative sulfide minerals rich in elements like S, Fe, Zn, and Pb, as well as InAs. The instrument's detection thresholds for these elements ranged from 100 ppm to 370 ppm: S (98 ppm), Fe (177 ppm), Co (159 ppm), Ni (175 ppm), Cu (200 ppm), Zn (265 ppm), As (204 ppm), and Pb (362 ppm).

Regarding the X-ray mapping of Cu (Kα), Fe (Kα), and S (Kα), an accelerating voltage of 20 kV was consistently applied, coupled with a beam current of 100 nanoamperes, a tightly-focused beam, and a dwell time of 50 milliseconds for each pixel to ensure comprehensive and detailed elemental distribution mapping.

LA-MC-ICP-MS Cu, Fe and S isotope measurements

The isotopic homogeneity of IGGCcp-1 grains was evaluated across mounts 1, 2, and 3 utilizing a 257 nm NWR-Femto laser ablation system coupled respectively with two different instruments – a Neptune Plus MC-ICP-MS dedicated to the measurement of Cu and Fe isotopic compositions, and another Neptune MC-ICP-MS specifically tailored for analyzing S isotopic profiles at IGGCAS.

During these precise measurements, we employed a single-spot ablation mode, which provided superior spatial resolution in comparison to the line scan mode. The spot diameters were set to 25 μm for Cu isotopes and 40 μm for Fe and S isotopes. The laser pulse repetition rates and energy densities were adjusted according to the specific isotopic analysis. For Cu isotopic analyses, a repetition rate of 4 Hz was maintained, in conjunction with an energy density of 0.1 J cm^{-2} at a consistent 3% energy output level. In the case of Fe isotopes, the parameters were tuned to a repetition rate of 8 Hz, delivering an energy density of around 0.14 J cm^{-2} at a 6% energy output. For S isotopes, to ensure optimal results, the repetition rate was escalated to 15 Hz due to their high ionized energy, while maintaining a comparable energy density of about 0.14 J cm^{-2}, also at a 6% output intensity.

For the MC-ICP-MS system, the Faraday cup arrangement was meticulously optimized. With regard to Cu isotopes, the focal point was on directing ion currents of ^{63}Cu and ^{65}Cu. In the specific scenario of Fe isotopes, the configuration was fine-tuned to capture ion beams encompassing ^{53}Cr, ^{54}Fe, ^{56}Fe, ^{57}Fe, and ^{58}Fe, as well as ^{60}Ni. Here, ^{53}Cr and ^{60}Ni strategically served as monitors to correct potential isobaric interferences on ^{54}Fe and ^{58}Fe measurements. Lastly, for the analysis of S isotopes, the setup was adapted to acquire ion beams of ^{32}S, ^{33}S, and ^{34}S.

Cu isotope measurements were conducted in low mass resolution mode, whereas Fe and S isotope measurements were performed in high mass resolution mode ($m/\Delta m \sim 8000$–9000) to resolve interferences from polyatomic ions such as $^{40}Ar^{16}O^+$, $^{40}Ar^{17}O^+$, $^{40}Ar^{14}N^+$, $^{16}O^{16}O^+$, $^{16}O^{17}O^+$, $^{17}O^{17}O^+$, $^{16}O^{18}O^+$, and $^{32}S^1H^+$ on Fe and S isotopes. Each spot analysis consisted of a block of 60 cycles with an integration time of 0.262 seconds per cycle. Detailed parameters were presented in ESI Table S1.†

Typical mean signal intensities were approximately 18 V for ^{63}Cu, 16 V for ^{56}Fe, and 12 V for ^{32}S. The analytical precision, represented by the relative standard error (RSE), was less than 0.002% for the $^{65}Cu/^{63}Cu$ ratio, 0.003% for the $^{56}Fe/^{54}Fe$ ratio, and 0.004% for the $^{34}S/^{32}S$ ratio in a single spot analysis. However, due to the low signal intensity (roughly 0.1 V) and poor precision (>0.01%, RSE), $^{33}S/^{32}S$ ratios were not used to assess S isotope homogeneity.

To rectify mass fractionation occurring during the analyses and accurately gauge potential isotopic variations between individual laser spot measurements and their immediate neighbors, we implemented the standard-sample-bracketing (SSB) method. In this process, each analyzed spot was considered a 'sample' and was systematically sandwiched between the preceding and succeeding spots acting as 'standards'. The isotope ratios were expressed as per mil deviations from the mean 'standards value' using the following formulae: $\delta^{65}Cu = [(^{65}Cu/^{63}Cu)_{sample}/\text{average of }(^{65}Cu/^{63}Cu)_{standards} - 1] \times 1000‰$, $\delta^{56}Fe = [(^{56}Fe/^{54}Fe)_{sample}/\text{average of }(^{56}Fe/^{54}Fe)_{standards} - 1] \times 1000‰$, $\delta^{57}Fe = [(^{57}Fe/^{54}Fe)_{sample}/\text{average of }(^{57}Fe/^{54}Fe)_{standards} - 1] \times 1000‰$, and $\delta^{34}S = [(^{34}S/^{32}S)_{sample}/\text{average of }(^{34}S/^{32}S)_{standards} - 1] \times 1000‰$.

This SSB methodology and optimized parameters were consistently adopted in the subsequent investigations of positional effects and matrix effects on the isotopic measurements.

SN-MC-ICP-MS Cu and Fe isotope measurements

Chemical procedures and measurements for Cu and Fe isotope compositions in chalcopyrite samples were adhered closely to the methodologies outlined in the works of Huang *et al.* (2017),[23] Huang *et al.* (2011),[24] and Liu *et al.* (2014).[25] These analyses were carried out using the solution nebulizer multi-collector inductively coupled plasma mass spectrometry (SN-MC-ICP-MS) technique at the CAS Key Laboratory of Crust-Mantle Materials and Environments, University of Science and Technology of China (USTC), Hefei, China, and the Isotope Geochemistry Laboratory of the China University of Geosciences (CUG), Beijing, China, respectively.

Chalcopyrite samples containing more than 2 μg Cu were digested in capped PFA beakers using a 3 : 1 volumetric mixture of doubly sub-distilled concentrated HF and HNO_3. Digestion took place overnight at approximately 100 °C on a hotplate. After samples were evaporated to dryness, 1 mL of doubly sub-distilled concentrated HCl was added to facilitate further thorough digestion.

To validate the feasibility of measuring Cu isotopic composition in chalcopyrite without a chemical column purification step, the resultant solution was divided into two equal portions. Both aliquots were evaporated to dryness. Subsequently, one aliquot was diluted with 2% (m/m) HNO_3 and prepared for direct isotope analysis. The other aliquot was diluted with 1 mL 6 mol L^{-1} HCl mixed with 0.001% H_2O_2 and then underwent an additional chemical column purification step specifically for Cu, which detailed in the Cu and Fe purification procedures section of the ESI.†

Cu isotopes were accurately measured using a Neptune Plus MC-ICP-MS in low-resolution mode. A block of analysis consisted of 30 cycles of data with an integration time of 4.194 s per cycle. The sensitivity of ^{63}Cu was about 30 V per μg g^{-1}. The SSB technique was used to correct the instrumental mass bias, and the reference material NIST976 served as the bracketing standard. The Cu isotopes of BCR-2 were measured alongside samples, and the obtained $\delta^{65}Cu_{NIST976}$ was 0.20 ± 0.03‰, which was consistent with the previously published data from Huang *et al.* (2017).[23]

Regarding the Fe isotope analysis, chalcopyrite samples containing about 50 μg of Fe were processed as follows: they were subjected to digestion in capped PFA beakers using a 3 : 1 volumetric mixture of doubly sub-distilled concentrated HF and HNO_3, and left to heat at about 100 °C on a hotplate overnight. Upon complete evaporation, the samples underwent further digestion with aqua regia.

To substantiate also the practicality of determining Fe isotopic composition in chalcopyrite without necessitating a chemical column purification process, the resulting solution was divided into two equal aliquots. Both aliquots were evaporated to dryness, accordingly one was diluted with 2% HNO_3 (m/m) for immediate isotope analysis, while the other was diluted with 1 mL of 6 mol L^{-1} HCl before proceeding to purification. And the procedure was detailed in the Cu and Fe purification procedures section of the ESI.†

Fe isotopes were determined using a Neptune Plus MC-ICP-MS in high resolution mode. The cup configuration was identical to the one employed in the aforementioned LA-MC-ICP-MS. The sensitivity of ^{56}Fe was about 6 V μg^{-1} g^{-1}. A block of analysis consisted of 30 cycles of data with an integration time of 4.194 s per cycle. The instrumental mass bias was corrected using the SSB method, and the bracketing standard was the reference material IRMM014. The Fe isotopes of BHVO-2 were measured alongside samples, and the $\delta^{56}Fe_{IRMM014}$ was 0.09 ± 0.03‰, which is consistent with the published data from Liu *et al.* (2014).[25]

EA-IRMS S isotope measurement

S isotope ratios ($^{34}S/^{32}S$) were determined at IGGCAS through the application of an Elemental Analyzer-Isotope Ratio Mass Spectrometry (EA-IRMS) technique. Precisely, around 300 micrograms of powdered chalcopyrite sample, combined with approximately 2.4 milligrams of V_2O_5 reagent, were carefully weighed into a tin capsule. This encapsulated mixture was subsequently inserted into a Flash HT 2000 high-temperature pyrolysis furnace, which was ingeniously connected *via* a Finnigan Conflo IV open-split interface to a Thermo Scientific DELTA V Advantage mass spectrometer.

In this sophisticated setup, the sulfide compounds underwent thermal conversion into SO_2, with helium functioning as the carrier gas throughout the process. Calibration of the S isotopes was accomplished by leveraging internationally recognized reference materials: IAEA S1 (with a $\delta^{34}S$ value of −0.30‰), IAEA S2 (having a $\delta^{34}S$ of 22.62‰), and IAEA S3 (with a $\delta^{34}S$ reading of −32.49‰).[26] The resulting $\delta^{34}S$ data were reported in accordance with the Vienna-Canyon Diablo Troilite (VCDT) scale benchmark. The reproducibility of the $\delta^{34}S$ measurements was falling within a range of ±0.60‰, which is expressed as two standard deviations (2SD).

S isotope analysis by SIMS

In order to delve deeper into the S isotopic composition of the IGGCcp-1 chalcopyrite specimen, meticulous cleaning and gold-coating procedures were performed on the mount 5. Subsequently, a systematic random selection of 25 particles was made for spot analysis using a CAMECA IMS 1280 secondary ion mass spectrometer (SIMS) at the IGGCAS. During the data collection phase, 32S⁻ and 34S⁻ ions were meticulously captured *via* dual Faraday cups-L2p and H1-each equipped with feedback resistors of 1×10^{10} Ω and 1×10^{12} Ω, respectively. Each selected spot underwent thirty measurement cycles, with each cycle integrating for 1 second. The other detailed parameters were similar to those applied in the reference by Xie *et al.* (2024).[27]

Typically, the count rate for $^{32}S^-$ ions reached about 9×10^8 counts per second. The internal precision of a single-spot $^{34}S/^{32}S$ ratio measurement was typically maintained at approximately 0.15‰ (2SE).

To monitor instrumental drift and assess mass fractionation, the IGGCcp-2 chalcopyrite grains served as a reference material, being measured after every third sample analysis. The EA-IRMS technique was employed to perform nine replicate analyses on the IGGCcp-2 sample, yielding a mean $\delta^{34}S_{VCDT}$ value of −0.08 ± 0.32‰ (2S, $N = 9$). This data was accessible within the 'Introduction of IGGCcp-2 chalcopyrite sample' section of the ESI.† This average value served as the reference value in calculating the instrumental mass fractionation correction for the IGGCcp-1 chalcopyrite sample using the formula: $\delta^{34}S_{final} = \delta^{34}S_{measured} + (\delta^{34}S_{ref.\ value\ of\ IGGCcp\text{-}2} - \text{mean of } \delta^{34}S_{measured\ value\ of\ IGGCcp\text{-}2})$.

Results and discussion

Chemical composition of IGGCcp-1

The elemental compositions, encompassing both major and trace elements, of chalcopyrite grains sourced from sample IGGCcp-1 were precisely determined utilizing EPMA. To assess the consistency of major element compositions across diverse grains, a systematic spot analysis was executed on a randomly selected set of ten grains, numbered consecutively from IGGCcp G01 to IGGCcp G10, with one analysis performed per individual grain. The results were tabulated in ESI Table S2.†

For a more profound investigation into the intra-grain compositional homogeneity, two additional grains, designated as IGGCcp G11 and IGGCcp G12, underwent extensive scrutiny. Each of these grains was subject to multiple spot analyses – with 20 spots measured on grain IGGCcp G11 and 19 spots on grain IGGCcp G12. These analyses strategically spanned the entirety of each grain, systematically crossing from edge to edge and passing through their central points to provide a comprehensive assessment. The detailed analytical results were presented in ESI Table S2.†

EPMA data derived from the examination of ten grains indicated a remarkable degree of homogeneity in the major element compositions of the chalcopyrite sample IGGCcp-1. Concentrations of Cu, Fe, and S exhibited a tight range of variation, oscillating between 33.5 to 34.2 wt% for Cu, 29.2 to 29.9 wt% for Fe, and 34.3 to 34.6 wt% for S, with mean values calculated as 33.8 ± 0.2 (1S) wt% for Cu, 29.7 ± 0.2 (1S) wt% for Fe, and 34.5 ± 0.1 (1S) wt% for S.

Additionally, the IGGCcp-1 chalcopyrite samples contained a minor amount of Co, averaging 0.93 ± 0.02 (1S) wt%. Pb was found at a low but discernible average concentration of 0.05 ± 0.03 (1S) wt%, while Ni, Zn and As levels were either below or close to the detection limits.

The meticulous 20 spot analyses conducted on the grain of IGGCcp G11 resulted in mean concentration values of 34.1 ± 0.1 (1S) wt% for Cu, 29.8 ± 0.1 (1S) wt% for Fe, 34.5 ± 0.1 (1S) wt% for S and 0.94 ± 0.01 (1S) wt% for Co, respectively. Parallelly, grain IGGCcp G12, after undergoing 19 spot analyses, displayed comparable average concentration values of 34.1 ± 0.1 (1S) wt% for Cu, 29.8 ± 0.1 (1S) wt% for Fe, 34.5 ± 0.1 (1S) wt% for S and 0.93 ± 0.01 (1S) wt% for Co. The consistent mean concentrations for these major elements across both grains suggested an absence of zonation in their major chemical compositions.

Furthermore, upon BSE imaging and Cu, Fe and S element mapping on a randomly chosen grain from mount 2 of the IGGCcp-1 sample, no evidence of internal growth zoning within the sample was detected. These findings were visually depicted in Fig. 2a–d, providing clear confirmation of the homogeneous distribution of these elements within the chalcopyrite grains.

LA-MC-ICP-MS Cu, Fe and S isotope measurements

Homogeneity on isotopic composition of IGGCcp-1. The LA-MC-ICP-MS technique was utilized to meticulously evaluate the homogeneity of Cu, Fe, and S isotope compositions of IGGCcp-1 chalcopyrite sample. To identify any possible isotopic zoning within individual grains and inter-grain disparities in Cu, Fe, and S isotope ratios, the grain-by-grain isotopic analysis strategy was performed on the chalcopyrite grains from mount 1, mount 2, and mount 3.

For larger grains, two to five spot analyses for Cu, Fe, or S isotopes were implemented from the edge to edge and through the center of each grain. On the other hand, for the smaller grains, a single spot analysis was executed per grain.

Specifically, on mount 1, a total of 85 spot analyses were carried out for the Cu isotopes; whereas, for mounts 2 and 3, there were respectively 59 Cu isotopic spot analyses conducted on each. Equal number of spot analysis was performed for the inspection of Fe and S isotopic homogeneity, with exactly 71 spot analyses for Fe isotopes and another 71 for S isotopes carried out across all sample mounts.

During the course of these analyses, the SSB technique was applied to correct for mass fractionation effects. The immediately preceding and succeeding spot analyses were arbitrarily designated as reference 'standards' for each given analysis point. The comprehensive results are tabulated in Table 1.

The measured δ^{65}Cu values in chalcopyrite grains from IGGCcp-1 showed a narrow range of variability. For mount 1, the δ^{65}Cu values spanned from −0.10‰ to 0.08‰, averaging at 0.00 ± 0.08‰ (2S, $N = 42$). In similar fashion, grains from mount 2 displayed a range from −0.09‰ to 0.08‰, setting at a mean of 0.00 ± 0.08‰ (2S, $N = 29$), and those from mount 3 varied from −0.07‰ to 0.07‰ with a mean of 0.00 ± 007‰ (2S, $N = 29$).

Regarding δ^{56}Fe values, the fluctuations were observed from −0.15‰ to 0.14‰ on mount 1, leading to an average of 0.01 ± 0.14‰ (2S, $N = 35$). On mount 2, the measured δ^{56}Fe values moved from −0.07‰ to 0.12‰, converging a mean of 0.00 ± 0.09‰ (2S, $N = 35$). Meanwhile, on mount 3, these values shifted from −0.10‰ to 0.10‰, yielding a mean of 0.00 ± 0.10‰ (2S, $N = 35$).

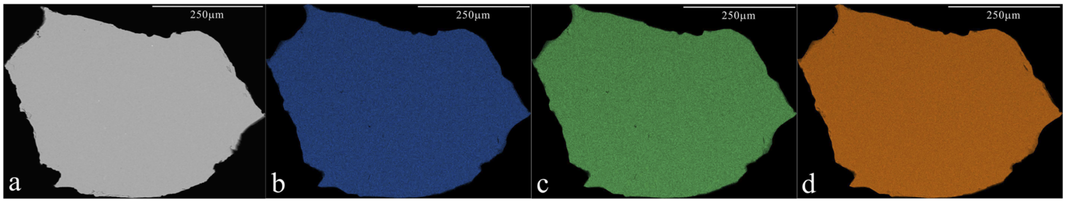

Fig. 2 The BSE imaging and Cu–Fe–S element mapping results of a randomly selected IGGCcp-1 chalcopyrite grain using an EPMA. (a) BSE imaging; (b) Cu content mapping; (c) Fe content mapping; (d) S content mapping.

Table 1 The results of homogeneity experiment for Cu, Fe and S isotope composition of IGGCcp-1

	Mount 1			Mount 2			Mount 3		
Analytical no.	δ^{65}Cu	δ^{56}Fe	δ^{34}S	δ^{65}Cu	δ^{56}Fe	δ^{34}S	δ^{65}Cu	δ^{56}Fe	δ^{34}S
1	−0.05	0.02	0.00	0.02	−0.05	−0.09	−0.01	0.10	0.03
2	0.03	0.10	−0.11	−0.04	0.09	0.15	−0.01	−0.04	0.15
3	0.02	−0.04	0.11	−0.03	0.02	−0.07	0.00	0.08	−0.01
4	−0.01	0.02	−0.09	0.01	−0.03	0.16	0.06	−0.03	−0.06
5	0.03	−0.10	0.13	−0.01	−0.04	−0.24	−0.03	−0.04	0.09
6	−0.03	0.04	−0.09	0.00	0.06	0.25	−0.02	0.06	−0.16
7	−0.01	0.04	−0.26	0.08	−0.03	−0.04	−0.01	0.01	−0.04
8	0.03	0.00	−0.28	0.03	0.03	0.10	−0.03	−0.02	0.06
9	0.01	−0.04	0.33	−0.04	0.00	−0.07	0.01	−0.05	0.06
10	−0.03	0.05	0.15	0.05	−0.04	0.07	−0.01	0.02	0.03
11	0.06	0.00	0.06	0.00	0.06	0.11	0.00	0.05	−0.09
12	−0.06	0.00	0.14	−0.01	−0.03	−0.12	0.02	−0.10	0.06
13	0.06	0.00	0.10	−0.02	0.02	−0.09	0.01	0.02	0.06
14	−0.02	−0.08	0.02	0.02	0.00	0.05	−0.02	0.07	−0.12
15	−0.05	0.12	0.01	0.00	−0.02	−0.16	−0.05	−0.04	0.10
16	0.07	0.01	−0.04	0.00	0.06	0.14	0.04	0.03	−0.07
17	0.02	0.14	0.05	−0.05	−0.06	−0.06	−0.03	−0.05	−0.17
18	−0.10	0.04	−0.06	0.04	−0.01	0.16	−0.03	0.01	0.22
19	0.05	0.05	−0.21	0.01	0.05	−0.06	−0.06	0.06	0.04
20	0.03	0.08	−0.05	0.03	−0.01	0.14	−0.01	−0.04	0.00
21	−0.07	−0.15	−0.06	0.04	−0.01	0.06	−0.01	−0.01	−0.03
22	0.08	0.03	−0.02	−0.02	0.05	0.03	0.06	0.00	0.01
23	0.00	−0.06	−0.03	−0.09	−0.07	−0.14	−0.05	−0.03	0.06
24	0.00	0.12	0.10	−0.02	0.01	−0.04	0.01	0.02	−0.02
25	−0.04	−0.07	−0.04	0.03	0.00	0.19	0.01	0.04	0.08
26	−0.01	−0.11	−0.02	−0.06	0.03	−0.27	0.07	−0.06	−0.09
27	−0.01	0.09	0.04	−0.06	−0.06	−0.07	0.00	0.05	0.11
28	0.04	0.05	0.02	0.04	0.04	0.15	0.06	−0.05	−0.10
29	0.05	0.05	0.07	−0.03	0.00	−0.20	−0.07	0.04	0.19
30	0.03	−0.06	−0.13		−0.03	0.21		−0.03	−0.10
31	0.00	0.03	−0.01		0.03	−0.09		−0.01	−0.09
32	0.00	−0.01	0.06		−0.03	−0.14		0.02	0.19
33	−0.02	−0.01	−0.03		0.02	0.07		−0.06	−0.10
34	−0.02	0.09	0.20		−0.06	−0.07		0.10	−0.10
35	−0.01	−0.08	0.02		0.12	−0.01		−0.08	0.01
36	0.00								
37	0.01								
38	−0.02								
39	0.01								
40	0.00								
41	0.05								
42	0.00								
Average	0.00	0.01	0.00	0.00	0.00	0.00	0.00	0.00	0.01
2S	0.08	0.14	0.24	0.08	0.09	0.27	0.07	0.10	0.20
t^a	0.41	0.87	0.11	0.30	0.41	0.02	0.51	0.13	0.35
$t_{\text{critical}}{}^b$	2.02	2.03	2.03	2.05	2.03	2.03	2.05	2.03	2.03

[a] The t-values were calculated using the formula: $t = \frac{|\overline{x} - \mu|}{S}\sqrt{n}$, where $\bar{x}$ represented the mean of observed deviations in copper, iron, or sulfur isotopic composition, which were calibrated against two adjacent ablated spots. S signified the standard deviation of these measurements, and n denoted the total number of values included in the analysis. μ here stood for the hypothetical population mean of the deviations in the isotopic composition of copper, iron, or sulfur. Under the assumption that the isotopic composition of the sample is homogeneous, and if the sole cause of variation is random error, then μ should theoretically equate to zero. This calculation helps assess whether the isotopic homogeneity hypothesis holds true for the IGGCcp-1 sample. [b] The critical t-values were calculated using the T.INV.2T function in Microsoft Excel under a two-tailed hypothesis at a significance level of 0.05.

Lastly, the δ^{34}S values also exhibited a relatively consistent pattern. At mount 1, the δ^{34}S readings oscillated from −0.28‰ to 0.33‰ with a mean of 0.00 ± 0.24‰ (2S, $N = 35$). For mount 2, the range was −0.27‰ to 0.27‰, averaging at 0.00 ± 0.27‰ (2S, $N = 35$), and on mount 3 the variation extended from −0.16‰ to 0.22‰, resulting in a mean of 0.01 ± 0.20‰ (2S, $N = 35$). Overall, these *in situ* analytical results indicated the variations in Cu, Fe and S isotopic compositions were remarkably small, thus suggesting that a high degree of homogeneity in the

Cu, Fe and S isotopic compositions across the different chalcopyrite grains from the IGGCcp-1 sample.

Our analytical approach enabled us to discern any potential differences in Cu, Fe, and S isotopic compositions both between grains (inter-grain) and within individual grains (intra-grain). Upon compiling and synthesizing the δ^{65}Cu, δ^{56}Fe, and δ^{34}S data points, we observed the following aggregate averages: for δ^{65}Cu, across mount 1, mount 2, and mount 3, the mean value was found to be 0.00 ± 0.08‰ (2S, $N = 100$); similarly, for δ^{56}Fe, the combined mean was 0.00 ± 0.11‰ (2S, $N = 105$); and for δ^{34}S, it was 0.00 ± 0.24‰ (2S, $N = 105$). These collective averages were graphically represented in Fig. 3a–c, respectively, offering a visual illustration of the isotopic homogeneity within and between the chalcopyrite grains sampled from the three distinct sample mounts.

A Student's *t*-test was conducted to further reinforce the assertion of isotopic homogeneity in the IGGCcp-1 chalcopyrite sample, which was a vital prerequisite for a reliable reference material. Assuming that IGGCcp-1 chalcopyrite has isotopically homogeneous properties influenced solely by random analytical

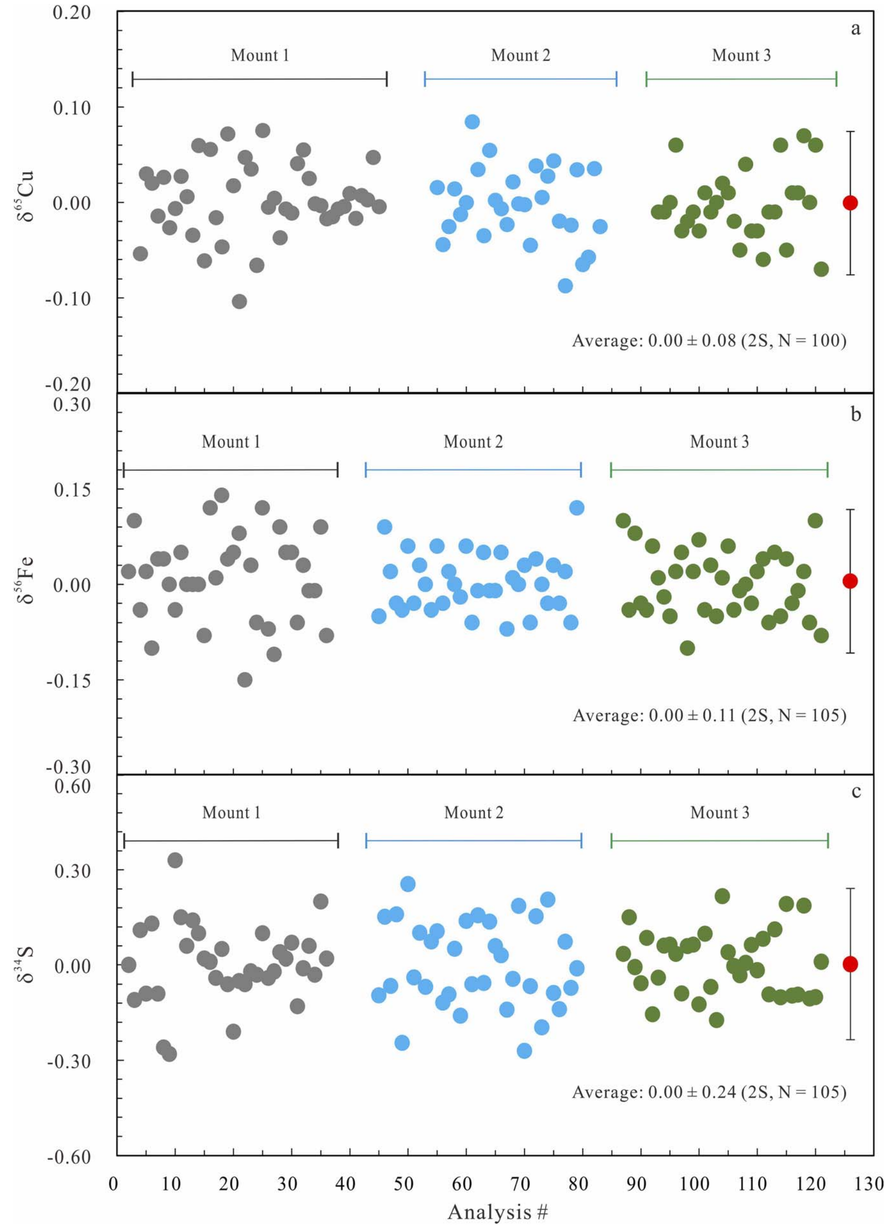

Fig. 3 The results of isotopic homogeneity experiments for IGGCcp-1 chalcopyrite using spot analysis by fs-LA-MC-ICP-MS. (a) Exhibited the δ^{65}Cu values, (b) showed the δ^{56}Fe values, and (c) presented the δ^{34}S values, all derived from random spot analyses on chalcopyrite grains sourced from mount 1, mount 2, and mount 3, and normalized against two neighboring ablated sites for calibration purposes. In the graph, the grey, blue, and green dots symbolized the individual data points gathered from mount 1, mount 2, and mount 3, respectively, whereas the red dots denoted the average values of these isotopic measurements. The error bars associated with each point represent the 2S uncertainties for these analytical data sets.

error, the population mean (μ) deviation in Cu, Fe, or S isotopic ratios when comparing two adjacent ablated spots should ideally equal zero.

Upon calculation, that *t*-values obtained for δ^{65}Cu were 0.41, 0.30, and 0.51 for grains from mounts 1, 2, and 3, respectively. Notably, all these values were appreciably lower than their corresponding critical *t*-values of 2.02, 2.05, and 2.05 at a significance level of 0.05, with degrees of freedom of 41, 28, and 28 for each mount. When considering δ^{56}Fe, the *t*-values stood at 0.87, 0.41, and 0.13 for mounts 1, 2, and 3, while for δ^{34}S, they were 0.11, 0.02, and 0.35, respectively. All these *t*-values were also less than the critical *t*-value of 2.03, again at a 0.05 significance level and with a degree of freedom of 34.

Collectively, these statistical outcomes demonstrated that there were no statistically significant differences in the Cu, Fe and S isotopic compositions of IGGCcp-1 chalcopyrite sample at a 95% confidence interval, as detailed in Table 1. Consequently, it can be reasonably deduced that the IGGCcp-1 chalcopyrite displays a high degree of isotopic homogeneity for Cu, Fe, and S.

Position effect. The observed position effect was attributed to the differential transport efficiency of ablated material stemming from the diverse isotopic compositions present in size-separated aerosol particles across various positions within the sample cell.[28,29] Notably, gas flow dynamics, which varied with distance from the gas inlet, played a crucial role in this transport efficiency.[28] In our more recent investigations, we had substantiated that this position effects occurring between dual mounts housed inside a TV2 sample chamber exerted a substantial impact on the precision and dependability of isotopic measurements for elements like Si, Zr, Fe, and S. This finding underscored the significance of accounting for such effects to enhance the overall quality of isotopic data derived from these analyses.[27,30]

In this study, we respectively conducted 21 spot analyses to measure the Cu isotope composition of IGGCcp-1 chalcopyrite grains located on mount 5 and mount 2 to assess the impact of position effects on Cu isotope composition measurements within a TV2 sample cell. To correct for mass fractionation, we utilized the SSB technique and used the IGGCcp-1 chalcopyrite grains on mount 4 as the calibrated reference material. This approach allowed us to evaluate the position effects between positions 5 or 2 and position 4. These deviations were denoted as $\delta^{65}\mathrm{Cu}_{5\ \mathrm{to}\ 4}$ and $\delta^{65}\mathrm{Cu}_{2\ \mathrm{to}\ 4}$, respectively.

Additionally, we also measured the Cu isotope compositions of IGGCcp-1 on mounts 1 and 3 with 21 of spot analysis for each mount. The IGGCcp-1 sample on mount 5 served as the calibrated reference material to examine the position effects between positions 3 or 1 and position 5. These deviations were expressed as $\delta^{65}\mathrm{Cu}_{3\ \mathrm{to}\ 5}$ and $\delta^{65}\mathrm{Cu}_{1\ \mathrm{to}\ 5}$, respectively.

In terms of spatial arrangement, positions 2 and 4 occupied horizontally adjacent spots in the central area, while positions 3 and 5 were horizontally aligned at the lower part of the setup. Positions 5 and 4 stood vertically next to each other on the right side, and positions 1 and 5 represented the most distant pair within the layout (refer to Fig. 1b).

Theoretically, if only random errors were present without any position effects, the deviation per mil values (expressed as $\delta^{65}\mathrm{Cu}_{1\ \mathrm{to}\ 5}$, $\delta^{65}\mathrm{Cu}_{2\ \mathrm{to}\ 4}$, $\delta^{65}\mathrm{Cu}_{3\ \mathrm{to}\ 5}$, and $\delta^{65}\mathrm{Cu}_{5\ \mathrm{to}\ 4}$) for IGGCcp-1 chalcopyrite at positions $x = (1, 2, 3, \text{and } 5 \text{ respectively})$ should be near zero. The average values obtained for $\delta^{65}\mathrm{Cu}_{5\ \mathrm{to}\ 4}$, $\delta^{65}\mathrm{Cu}_{2\ \mathrm{to}\ 4}$, $\delta^{65}\mathrm{Cu}_{3\ \mathrm{to}\ 5}$, and $\delta^{65}\mathrm{Cu}_{1\ \mathrm{to}\ 5}$ were 0.03 ± 0.04 (2S, $N = 21$), 0.01 ± 0.03 (2S, $N = 21$), −0.16 ± 0.05 (2S, $N = 21$), and 0.18 ± 0.08 (2S, $N = 21$), respectively. These results were presented in ESI Table S3.†

To evaluate the significance of the position effect among these measurement positions, a Student's *t*-test was conducted. The calculated *t*-value for $\delta^{65}\mathrm{Cu}_{2\ \mathrm{to}\ 4}$ was 1.86, which was lower than the critical *t*-value of 2.09 at a 95% confidence interval. This suggested that the position effect of Cu isotopes between positions 2 and 4 was not statistically significant, similar to the Fe and S isotopic position effects reported by Xie *et al.* (2024).[27] However, the calculated *t*-values for $\delta^{65}\mathrm{Cu}_{5\ \mathrm{to}\ 4}$, $\delta^{65}\mathrm{Cu}_{3\ \mathrm{to}\ 5}$, and $\delta^{65}\mathrm{Cu}_{1\ \mathrm{to}\ 5}$ were 3.00, 15.00, and 10.66, respectively, all higher than the critical *t*-value of 2.09 at a 95% confidence interval. This implied that the position effects between positions 5 and 4, 3 and 5, and 1 and 5 exhibited statistically significant differences at a 95% confidence interval (as shown in ESI Table S3†).

TV2 sample cell was designed with helium gas feeding from dual sides, accommodating a centrally-positioned sample mount tray with a small cup situated directly above it. During the process, the laser beam targeted the sample positioned at the base of the small cup, ablating it into an aerosol which was then transported out of the cup.

The integration of these newly acquired δ^{65}Cu results with the previously reported δ^{56}Fe and δ^{34}S data from Xie *et al.* (2024)[27] highlighted the intricacy of the gas flow dynamics within the TV2 system. This complexity underscored the paramount importance of conducting a thorough investigation for positional effects within the chamber, particularly regarding the locations of both reference materials and samples. Such meticulous attention to detail was essential prior to carrying out *in situ* Cu and other metal isotope measurements using LA-MC-ICP-MS, to ensure accurate and reproducible results.

Isotope composition of IGGCcp-1

Cu isotope composition. The Cu isotope composition measurements of twelve parallel samples randomly selected from IGGCcp-1 chalcopyrite grains were independently carried out using SN-MC-ICP-MS at both USTC and CUG. The $\delta^{65}\mathrm{Cu}_{\mathrm{NIST976}}$ results were tabulated in Table 2.

At USTC, six parallel samples were divided into two categories: three underwent chemical chromatography after acid dissolution, while the other three did not. The obtained $\delta^{65}\mathrm{Cu}_{\mathrm{NIST976}}$ values following the chemical chromatography process ranged from 0.44 to 0.46‰ with a weighted average of 0.45 ± 0.03‰ (2S, $N = 6$). In contrast, the $\delta^{65}\mathrm{Cu}_{\mathrm{NIST976}}$ values without the chromatography step varied from 0.43 to 0.45‰, averaging at 0.44 ± 0.04‰ (2S, $N = 6$). The average values of each set of the two datasets showed consistency within analytical uncertainties. A Student's *t*-test was further conducted to assess the difference between the chemical processes involving

Table 2 Cu isotopic composition of IGGCcp-1measured by SN-MC-ICP-MS

Sample no.	$\delta^{65}\mathrm{Cu}_{\mathrm{NIST976}}$	2S	N	With/without chemical chromatography procedure
Analyzed at USTC				
1	0.44	0.02	2	With
2	0.46	0.002	2	With
3	0.46	0.01	2	With
Weighted average[a]	0.45	0.03	6	
4	0.44	0.03	2	Without
5	0.45	0.01	2	Without
6	0.43	0.04	2	Without
Weighted average[a]	0.44	0.04	6	
t[b]	0.67			
t_{critical}[b]	2.78			
Weighted average[a]	0.45	0.04	12	
Analyzed at CUG				
7	0.41	0.04	3	With
8	0.42	0.04	3	With
Weighted average[a]	0.42	0.04	6	
9	0.43	0.03	3	Without
10	0.43	0.02	3	Without
11	0.44	0.02	3	Without
12	0.44	0.02	3	Without
Weighted average[a]	0.43	0.02	12	
t[b]	1.86			
t_{critical}[b]	2.78			
Weighted average[a]	0.43	0.04	18	
t[b]	0.13			
t_{critical}[b]	2.23			
Weighted average[a]	0.43	0.05	30	

[a] The weighted average of Cu isotopic composition measurements for z parallel IGGCcp-1 chalcopyrite samples and the corresponding standard deviation were calculated using the following formulas: $\overline{X}=\frac{\sum_{i=m}^{n}N_i\overline{X_i}}{\sum_{i=m}^{n}N_i}$ and $S=\sqrt{\frac{\sum_{i=m}^{n}(N_i-1)S_i^2+\sum_{i=m}^{n}N_i(\overline{X_i}-\overline{X})^2}{\sum_{i=m}^{n}N_i-z}}$, respectively. Here, N_i and $\overline{X_i}$ represented the times of measurement and the mean of the N_i measured values for the ith parallel sample, respectively. S_i denoted the standard deviation of the mean $(\overline{X_i})$ calculated from the N_i measurements for the ith sample. Regarding the data analysis conducted at USTC on IGGCcp-1 chalcopyrite samples: when chemical chromatography was applied, m and n took the values 1 and 3 respectively; conversely, for those samples not treated with chemical chromatography, m and n were set to 4 and 6 respectively. Considering all data from USTC, regardless of treatment, m was assigned 1 and n was 6. In the case of chalcopyrite samples analyzed at CUG, when chemical chromatography was used, m and n had the values 7 and 8 correspondingly; whereas for those without the chemical chromatography procedure, m and n were set to 9 and 12 respectively. For all data obtained from CUG, irrespective of the treatment method, m was assigned 7 and n was 12. For all combined data from the 12 parallel IGGCcp-1 chalcopyrite samples analyzed at both USTC and CUG, m was set as 1 and n was 12. [b] The pooled standard deviation and t-values were calculated using the following formulas: Pooled $S=\sqrt{\frac{\sum_{i=n}^{m}(\overline{X_i}-\overline{X_a})^2+\sum_{i=o}^{p}(\overline{X_i}-\overline{X_b})^2}{z_a+z_b-2}}$ and $t=\frac{\left|\overline{X_a}-\overline{X_b}\right|}{\text{Pooled }S}\sqrt{\frac{z_a z_b}{z_a+z_b}}$, respectively. Here, $\overline{X_i}$ represented the mean of measured values for the Cu isotopic composition in the ith sample. Within the dataset analyzed at USTC, z_a and z_b indicated the quantities of parallel samples that underwent treatment with or without a chemical chromatography step, respectively. The weighted averages for these two groups were given as $\overline{X_a}$ for those treated with chromatography and $\overline{X_b}$ for those without. Specifically, in this case, m and n were set to 1 and 3, whereas o and p had values of 4 and 6, respectively. For the data analyzed at CUG, z_a and z_b again represented the quantities of parallel samples subjected to either chemical chromatography or no such treatment. The respective weighted averages for these two groups were given as $\overline{X_a}$ and $\overline{X_b}$. Specifically, in this case, m and n were set to 7 and 8, whereas o and p had values of 9 and 12, respectively. Considering all chalcopyrite sample data collectively from both USTC and CUG, z_a and z_b signified the total quantities of parallel samples analyzed across the two institutions. Their corresponding weighted averages for each group were once more designated as $\overline{X_a}$ and $\overline{X_b}$. In this comprehensive case, m and n values were established as 1 and 6, while o and p equated to 7 and 12, respectively. The critical t-values were calculated using Excel's T.INV.2T function, applying a significance level of 0.05 under a two-tailed hypothesis.

and excluding chromatography for Cu isotope composition measurements. The calculated t-value for the averages of $\delta^{65}\mathrm{Cu}_{\mathrm{NIST976}}$ was 0.67, which was less than the critical t-value of 2.78 at a 95% confidence level, indicating no statistically significant difference or systematic error between the datasets. Therefore, it was reasonable to combine these two sets of Cu isotopic data, resulting in an overall average of 0.45 ± 0.04‰ (2S, $N = 12$).

Similarly, at CUG, six parallel samples were split into two groups; two were processed with chemical chromatography post-acid dissolution, and the rest were not. The $\delta^{65}\mathrm{Cu}_{\mathrm{NIST976}}$ values with chromatography ranged from 0.41 to 0.42‰, having a weighted average of 0.42 ± 0.04‰ (2S, $N = 6$), whereas those without chromatography spanned from 0.43 to 0.44‰, with a mean of 0.43 ± 0.02‰ (2S, $N = 12$). Again, the mean values from both groups were consistent within analytical uncertainty margins. Zhang *et al.* (2020) revealed that matrix interference of Co and Fe on Cu isotopic measurements were negligible when the molar ratio of Fe (or Co) to Cu was ≤2.[31] while the matrix elements in chalcopyrite samples without chromatography fell below the threshold, the matrix influence on Cu isotopic analysis was neglected. Applying Student's *t*-test to evaluate the difference in the chemical treatments, the calculated *t*-value for the average of $\delta^{65}\mathrm{Cu}_{\mathrm{NIST976}}$ was 1.86, which was lower than the critical value of 2.78 at the 95% confidence level, signifying no statistical disparity or systemic error between these data sets. Thus, merging these two groups' Cu isotopic data was justified, leading to a combined average of 0.43 ± 0.04‰ (2S, $N = 18$).

Notably, there appeared to be slight discrepancies between the average values measured at USTC and CUG. Consequently, it was essential to perform *F*-test and *t*-test analyses to evaluate precision differences and system errors before combining the datasets. The calculated *F*-value for the standard deviations of $\delta^{65}\mathrm{Cu}_{\mathrm{NIST976}}$ was 1.12, which fell below the critical value of 5.05 at the 95% confidence level, suggesting that there was no statistically significant difference in precision between the two datasets. Additionally, the *t*-values calculated for the average of $\delta^{65}\mathrm{Cu}_{\mathrm{NIST976}}$ was 0.13, which was also lower than the critical value of 2.23 at the same confidence level. This indicated no statistically significant difference or systematic error between the two sets of data. Hence, it was valid to merge these Cu isotopic data, yielding a weighted average value of 0.43 ± 0.05‰ (2S, $N = 30$). Based on this, we proposed this value as the Cu isotopic reference values for IGGCcp-1.

Fe isotope composition. Fe isotope compositions of six randomly chosen parallel samples from IGGCcp-1 chalcopyrite grains were analyzed at USTC, and the results were presented in Table 3.

These six parallel samples were divided into two categories: three underwent chemical chromatography following acid dissolution, while the other three did not undergo this process. The obtained $\delta^{56}\mathrm{Fe}_{\mathrm{IRMM\text{-}014}}$ values after chemical chromatography ranged from −0.23 to −0.23‰, with a weighted mean of −0.23 ± 0.01‰ (2S, $N = 9$). Similarly, the corresponding $\delta^{57}\mathrm{Fe}_{\mathrm{IRMM\text{-}014}}$ values spanned from −0.34 to −0.36‰, averaging at −0.35 ± 0.09‰ (2S, $N = 9$). In contrast, without the chromatography step, the $\delta^{56}\mathrm{Fe}_{\mathrm{IRMM\text{-}014}}$ values varied from −0.22 to −0.25‰, resulting in a weighted average of −0.24 ± 0.05‰ (2S,

Table 3 Fe isotopic composition of IGGCcp-1measured by SN-MC-ICP-MS

Sample no.	$\delta^{56}\mathrm{Fe}_{\mathrm{IRMM\text{-}014}}$	2S	$\delta^{57}\mathrm{Fe}_{\mathrm{IRMM\text{-}014}}$	2S	N	With/without chemical chromatography procedure
Analyzed by USTC						
1	−0.23	0.02	−0.34	0.09	3	With
2	−0.23	0.01	−0.36	0.10	3	With
3	−0.23	0.01	−0.35	0.06	3	With
Weighted average[a]	−0.23	0.01	−0.35	0.09	9	
4	−0.22	0.01	−0.34	0.03	3	Without
5	−0.25	0.05	−0.42	0.05	3	Without
6	−0.25	0.01	−0.35	0.03	3	Without
Weighted average[a]	−0.24	0.05	−0.37	0.09	9	
t[b]	0.60		0.67			
t_{critical}[b]	2.78					
Weighted average[a]	−0.24	0.04	−0.36	0.09	18	Merging two sets of data above

[a] The weighted average of Fe isotopic composition measurements for z parallel IGGCcp-1 chalcopyrite samples and the corresponding standard deviation were calculated using the following formulas: $\overline{X} = \frac{\sum_{i=m}^{n} N_i\overline{X_i}}{\sum_{i=m}^{n} N_i}$ and $S = \sqrt{\frac{\sum_{i=m}^{n}(N_i - 1){S_i}^2 + \sum_{i=m}^{n} N_i(\overline{X_i} - \overline{X})^2}{\sum_{i=m}^{n} N_i - z}}$, respectively. Here, N_i represented the times of the Fe isotopic measurement for the ith parallel, while $\overline{X_i}$ was the mean of the N_i measured values. S_i denoted the standard deviation of the mean $(\overline{X_i})$ calculated from N_i measurements of the *i*th sample. For data obtained with chemical chromatography procedure, m and n took the values of 1 and 3, respectively, conversely, for data without chemical chromatography, m and n were set to 4 and 6. However, when considering both sets of data together, regardless of whether chemical chromatography was used or not, m was assigned a value of 1 and n was given a value of 6. [b] The *t*-values were calculated using the following formula: $t = \frac{\left|\overline{X_{\mathrm{a}}} - \overline{X_{\mathrm{b}}}\right|}{\text{Pooled } S}\sqrt{\frac{z_{\mathrm{a}}z_{\mathrm{b}}}{z_{\mathrm{a}} + z_{\mathrm{b}}}}$. Here, Pooled S is calculated as: Pooled $S = \sqrt{\frac{\sum_{i=1}^{3}(\overline{X_i} - \overline{X_{\mathrm{a}}})^2 + \sum_{i=4}^{6}(\overline{X_i} - \overline{X_{\mathrm{b}}})^2}{z_{\mathrm{a}} + z_{\mathrm{b}} - 2}}$. In this context, $\overline{X_i}$ represented the mean of measured values for the Fe isotopic composition in the ith sample. z_{a} and z_{b} indicated the quantities of parallel samples that underwent treatment with or without a chemical chromatography step, respectively. The weighted averages for these two groups were given as $\overline{X_{\mathrm{a}}}$ for those treated with chromatography and $\overline{X_{\mathrm{b}}}$ for those without. The critical *t*-values were determined by utilizing the T.INV.2T function in Excel under a two-tailed hypothesis at a significance level of 0.05, with a degree of freedom of 5.

$N = 9$), and the $\delta^{57}\mathrm{Fe}_{\mathrm{IRMM\text{-}014}}$ values fluctuated between −0.34 to −0.42‰, leading to a mean of −0.37 ± 0.09‰ (2S, $N = 9$). The mean values for each set within these two datasets exhibited consistency within analytical uncertainties. He *et al.* (2014) showed that matrix effects on Fe isotopic measurements were negligible when the concentration ratio of Co to Fe was ≤1 and Cu to Fe was ≤2.[32] As the matrix elements in chalcopyrite samples without chromatography fell below these thresholds, the impact on Fe isotopic analysis was insignificant.

To further investigate any differences due to the inclusion or exclusion of chemical chromatography in the Fe isotope composition measurements, a Student's *t*-test was also performed. The calculated *t*-values for the averages of $\delta^{56}\mathrm{Fe}_{\mathrm{IRMM\text{-}014}}$ and $\delta^{57}\mathrm{Fe}_{\mathrm{IRMM\text{-}014}}$ were 0.60 and 0.67, respectively, both of which were lower than the critical value of 2.78 at a 95% confidence level, and the results were tabulated in Table 3. This suggested that there was no statistically significant difference or systematic error between the datasets. As such, it was justifiable to merge these two sets of Fe isotopic data. Upon combining, the overall weighted averages were found to be −0.24 ± 0.04‰ (2S, $N = 18$) for $\delta^{56}\mathrm{Fe}_{\mathrm{IRMM\text{-}014}}$ and -0.36 ± 0.09‰ (2S, $N = 18$) for $\delta^{57}\mathrm{Fe}_{\mathrm{IRMM\text{-}014}}$.

Table 4 S isotopic composition of IGGCcp-1 measured by three methods

	δ^{34}S		
Analysis no.	EA-IRMS	fs-LA-MC-ICP-MS[a]	SIMS[a]
1	−0.06	−0.09	−0.56
2	−0.44	−0.06	−0.41
3	−0.41	−0.11	−0.62
4	−0.31	−0.13	−0.62
5	−0.35	−0.19	−0.49
6	−0.37	−0.14	−0.25
7	−0.37	−0.10	−0.32
8	−0.08	0.01	−0.46
9	−0.11	−0.18	−0.35
10	−0.32	−0.21	−0.28
11		−0.01	−0.64
12		0.06	−0.20
13		−0.04	−0.32
14		−0.10	−0.30
15		−0.17	−0.20
16		−0.06	−0.30
17		−0.08	−0.34
18		−0.23	−0.34
19		−0.20	−0.41
20		−0.10	−0.32
21			−0.31
22			−0.51
23			−0.50
24			−0.57
25			−0.45
Average	−0.28	−0.11	−0.40
2S	0.29	0.16	0.27

[a] IGGCcp-2 served as a reference material in the determination of sulfur isotopes *via* both SIMS and fs-LA-MC-ICP-MS methodologies. The comprehensive isotopic compositions of S, Cu, and Fe in the IGGCcp-2 sample are meticulously documented in Tables S4–S6, respectively, within the ESI.

S isotope composition. The S isotope composition of the IGGCcp-1 sample was determined using three distinct methodologies at the IGGCAS. The $\delta^{34}\mathrm{S}_{\mathrm{VCDT}}$ values obtained through EA-IRMS technique for a set of ten parallel samples ranged from −0.44 to −0.06‰, with an average value of −0.28 ± 0.29‰ (2S, $N = 10$).

Additionally, 25 randomly chosen chalcopyrite grains were subjected to S isotope ratio measurement *via* SIMS, resulting in $\delta^{34}\mathrm{S}_{\mathrm{VCDT}}$ values that varied between −0.64 and −0.20‰, with a mean of −0.40 ± 0.27‰ (2S, $N = 25$). Similarly, twenty randomly selected chalcopyrite grains were used to measure S isotopes with LA-MC-ICP-MS, which produced $\delta^{34}\mathrm{S}_{\mathrm{VCDT}}$ values ranging from −0.23 to −0.01‰, averaging at −0.11 ± 0.16‰.

These outcomes showed consistency within their respective uncertainties and were summarized in Table 4. Given the EA-IRMS technique's long-term precision of approximately 0.60‰ (2SD) for δ^{34}S measurements of chalcopyrite samples and considering only ten parallel chalcopyrite samples were analyzed, we proposed that the reference $\delta^{34}\mathrm{S}_{\mathrm{VCDT}}$ value for IGGCcp-1 should be estimated as −0.28 ± 0.60‰ (2SD).

Notably, the S isotope composition of IGGCcp-1 contrasted with that of another chalcopyrite sample, HTS4-6, which was collected from the same Hongtoushan copper–zinc deposit and studied by Li *et al.* (2020),[11] where it exhibited a δ^{34}S value of 0.63 ± 0.16‰. These discrepancies led us to define this chalcopyrite sample as IGGCcp-1.

Conclusions

In this study, an exhaustive examination of IGGCcp-1 chalcopyrite revealed uniform distribution of its major elements with weight percentages of Cu at 33.8 ± 0.2 (1S), Fe at 29.7 ± 0.0.2 (1S), S at 34.5 ± 0.1 (1S), and Co at 0.93 ± 0.02 (1S). Furthermore, employing LA-MC-ICP-MS analyses on three mounts, high precise data were obtained for δ^{65}Cu, δ^{56}Fe, and δ^{34}S at 0.08‰ (2S), 0.11‰ (2S), and 0.24‰ (2S), respectively. The rigorous precision of these isotope ratios, coupled with the outcomes of the Student's *t*-test, yielded excellent homogeneity in Cu, Fe, and S isotopes within IGGCcp-1. IGGCcp-1 demonstrated the excellent potential as the reference material for calibration, quality control, and validation in the field of *in situ* micro-analysis of chalcopyrite.

Based on these findings, we proposed adopting a $\delta^{65}\mathrm{Cu}_{\mathrm{NIST976}}$ value of 0.43 ± 0.05‰ (2S) and a $\delta^{34}\mathrm{S}_{\mathrm{VCDT}}$ value of −0.28 ± 0.60‰ (2S), while also recommending the use of the $\delta^{56}\mathrm{Fe}_{\mathrm{IRMM\text{-}014}}$ and $\delta^{57}\mathrm{Fe}_{\mathrm{IRMM\text{-}014}}$ values of −0.24 ± 0.04‰ (2S) and −0.36 ± 0.09‰ (2S), respectively, as benchmark values for IGGCcp-1.

We highlighted the significant influence of position effects within the TV2 sample chamber, particularly on Cu isotopic data accuracy. We strongly recommended a thorough evaluation of these effects in regions containing both reference materials and samples before Cu isotope determinations using LA-MC-ICP-MS.

Given the multi-stage genesis of many sulfide deposits, it's essential to recognize that aerosols ablated from various zones on a zoned chalcopyrite grain or even those originating from seemingly homogeneous smaller grains could represent different mineralization phases. The isotopically well-characterized IGGCcp-1 served as a valuable reference material for the future simultaneous measurement of Cu, Fe, and S isotopes in chalcopyrite using a single laser spot analysis through the LA-MC-ICP-MSs technique.

Data availability

The data that backs up this article is presented in Tables 1–4, while additional data has been appended in the ESI.†

Author contributions

Lie-Wen Xie conceptualized and designed the project, executed the experimental procedures, and drafted the original manuscript. Hong-Rui Fan contributed the IGGCcp-1 sample. Hui-Min Yu jointly performed the solution MC-ICP-MS experiments to analyze Cu and Fe isotopes and descripted the analytical method. Chao Huang supplied the data processing software and offered continuous technical assistance throughout the project. Lei Xu, Yue-Heng Yang, Shi-Tou Wu, and Hao Wang collectively provided essential technical support specifically for the fs-LA-MC-ICP-MS analyses. Each author made significant contributions by offering constructive feedback that enriched the overall quality and substance of the paper.

Conflicts of interest

There are no conflicts of interest to declare.

Acknowledgements

We would like to express our profound gratitude to Yiwen Lv for her exceptional expertise in conducting Cu and Fe isotopic measurements using the SN-MC-ICP-MS technique. Our heartfelt thanks also extend to Guo-Qiang Tang and Lian-Jun Feng, who kindly and generously provided their invaluable assistance by conducting S isotopic measurements using SIMS and EA-IRMS, respectively. We are equally appreciative of Qian Mao's professional prowess in meticulously performing element content assessments through EPMA. We are deeply indebted to Professor Ke-Zhang Qin for his gracious provision of the invaluable IGGCcp-2 chalcopyrite specimen, which significantly enriched our research. Furthermore, we extend our sincere appreciation to Hong-Xia Ma for her indispensable support in the meticulous preparation of samples, a vital contribution that greatly facilitated our study. We also appreciate two anonymous reviewers for their critical and insightful comments that greatly improved this manuscript. This research was jointly supported by the National Key Research and Development Program of China under Grant No. 2018YFA0702600 and the National Natural Science Foundation of China under Grant No. 41473012.

References

1 S. Graham, N. Pearson, S. Jackson, W. Griffin and S. Y. O'Reilly, *Chem. Geol.*, 2004, **207**, 147–169.
2 W. Li, S. E. Jackson, N. J. Pearson and S. Graham, *Geochim. Cosmochim. Acta*, 2010, **74**, 4078–4096.
3 B. Zhu, H. F. Zhang, P. Shen, B. X. Su, Y. Xiao and Y. S. He, *Ore Geol. Rev.*, 2018, **101**, 803–818.
4 Q. Shu, J. Deng, Z. Chang, Q. Wang, X. Niu, K. Xing, X. Sun, Z. Zhang, Q. Zeng, H. Zhao and F. Yu, *Econ. Geol.*, 2024, **119**, 1–22.
5 G. Markl, Y. Lahaye and G. Schwinn, *Geochim. Cosmochim. Acta*, 2006, **70**, 4215–4228.
6 C. LaFlamme, L. Martin, H. Jeon, S. M. Reddy, V. Selvaraja, S. Caruso, T. H. Bui, M. P. Roberts, F. Voute, S. Hagemann, D. Wacey, S. Littman, B. Wing, M. Fiorentini and M. R. Kilburn, *Chem. Geol.*, 2016, **444**, 1–15.
7 Z. Bao, K. Chen, C. Zong and H. Yuan, *J. Anal. At. Spectrom.*, 2021, **36**, 1657–1665.
8 H. R. Kuhn, N. J. Pearson and S. E. Jackson, *J. Anal. At. Spectrom.*, 2007, **22**, 547–552.
9 L. Chen, Y. T. Feng, H. M. Yu, L. Li, X. Ding, W. Zhang, J. T. Kang and X. H. Li, *At. Spectrosc.*, 2023, **44**, 14–23.
10 Y. Fang, H. M. Yu, L. W. Xie, S. Bin Fang, F. Huang and W. Y. Li, *J. Anal. At. Spectrom.*, 2023, **38**, 1626–1633.
11 R. Li, X. P. Xia, H. Chen, N. Wu, T. Zhao, C. Lai, Q. Yang and Y. Zhang, *Geostand. Geoanal. Res.*, 2020, **44**, 485–500.
12 Z. Bao, L. Chen, C. Zong, H. Yuan, K. Chen and M. Dai, *Int. J. Mass Spectrom.*, 2017, **421**, 255–262.
13 L. Chen, K. Chen, Z. Bao, P. Liang, T. Sun and H. Yuan, *J. Anal. At. Spectrom.*, 2017, **32**, 107–116.
14 Y. Feng, W. Zhang, Z. Hu, T. Luo, M. Li, Y. Liu, H. Liu and Q. Li, *J. Anal. At. Spectrom.*, 2022, **37**, 551–562.
15 K. Chen, Z. Bao, P. Liang, X. Nie, C. Zong and H. Yuan, *Spectrochim. Acta, Part B*, 2022, **188**, 106344.
16 D. E. Crowe and R. G. Vaughan, *Am. Mineral.*, 1996, **81**, 187–189.
17 Y. Kitayama, E. Thomassot, J. O'Neil and B. A. Wing, *Earth Planet. Sci. Lett.*, 2012, **355–356**, 271–282.
18 Y. Feng, W. Zhang, Z. Hu, T. Luo, Q. Li and J. Liu, *Geostand. Geoanal. Res.*, 2024, **48**, 227–244.
19 Y. Chen, L. Chen, G. Tang, Z. Bao, Z. Cui, X. Qiu, Z. Q. Chen, J. Gu, S. Dong and J. Gao, *At. Spectrosc.*, 2023, **44**, 131–141.
20 W. Yang, W. Zhang, Z. Hu, L. Zhou, S. A. Liu, X. Qiu and X. Tong, *Rapid Commun. Mass Spectrom.*, 2023, **37**, 9538.
21 L. Gu, Y. Zheng, X. Tang, K. Zaw, F. Della-Pasque, C. Wu, Z. Tian, J. Lu, P. Ni, X. Li, F. Yang and X. Wang, *Ore Geol. Rev.*, 2007, **30**, 1–29.
22 L. H. Li, H. R. Fan, Z. J. Qiu, K. F. Yang, J. Han and G. Zhao, *Ore Geol. Rev.*, 2022, **145**, 104885.
23 J. Huang, F. Huang, Z. Wang, X. Zhang and H. Yu, *Geochim. Cosmochim. Acta*, 2017, **211**, 48–63.
24 F. Huang, Z. Zhang, C. C. Lundstrom and X. Zhi, *Geochim. Cosmochim. Acta*, 2011, **75**, 3318–3334.
25 S. A. Liu, D. Li, S. Li, F. Z. Teng, S. Ke, Y. He and Y. Lu, *J. Anal. At. Spectrom.*, 2014, **29**, 122–133.

26 J. L. Mann, R. D. Vocke and W. R. Kelly, *Rapid Commun. Mass Spectrom.*, 2009, **23**, 1116–1124.

27 L. W. Xie, X. J. Wang, H. M. Yu, J. F. Gao, L. Xu, C. Huang, G. Q. Tang, Q. Mao, L. J. Feng, Y. H. Yang, S. T. Wu and H. Wang, *J. Anal. At. Spectrom.*, 2024, **39**, 723–734.

28 L. W. Xie, Q. Z. Yin, J. H. Yang, F. Y. Wu and Y. H. Yang, *J. Anal. At. Spectrom.*, 2011, **26**, 1773–1780.

29 X. Y. Zheng, B. L. Beard, S. Lee, T. R. Reddy, H. Xu and C. M. Johnson, *Chem. Geol.*, 2017, **450**, 235–247.

30 C. Huang, H. Wang, H. M. Yu, L. P. Feng, L. W. Xie, Y. H. Yang, S. T. Wu, L. Xu and J. H. Yang, *J. Anal. At. Spectrom.*, 2021, **36**, 2192–2201.

31 Y. Zhang, Z. Bao, N. Lv, K. Chen, C. Zong and H. Yuan, *Front. Chem.*, 2020, **8**, 609.

32 Y. He, S. Ke, F. Z. Teng, T. Wang, H. Wu, Y. Lu and S. Li, *Geostand. Geoanal. Res.*, 2015, **39**, 341–356.